Origin for Ellipticity of High-Order Harmonics Generated in Atomic Gases and the Sublaser-Cycle Evolution of Harmonic Polarization

V. V. Strelkov,[1,*] A. A. Gonoskov,[2] I. A. Gonoskov,[2] and M. Yu. Ryabikin[2]

[1]*General Physics Institute of the Russian Academy of Sciences, 38 Vavilova st., Moscow 119991, Russia*

[2]*Institute of Applied Physics of the Russian Academy of Sciences, 46 Ulyanov st., Nizhny Novgorod 603950, Russia*

(Received 2 March 2011; published 18 July 2011)

We investigate numerically and analytically the polarization properties of high-order harmonics generated by an atom in intense elliptically polarized laser field. The offset angle of the harmonic polarization ellipse can be well described with the semiclassic ''simple-man'' high-harmonic generation model. The harmonic ellipticity itself, however, can be hardly understood within this model. We show that this ellipticity originates from quantum-mechanical uncertainty of the electron motion. We develop a theoretical approach describing this ellipticity and, more generally, the time evolution of the high-harmonic polarization state within the laser cycle. The analytical results are verified with the exact numerical solution; to make the comparison accurately, we develop a specific technique for separating the contributions of quantum paths in the numerical calculation.

DOI: 10.1103/PhysRevLett.107.043902 PACS numbers: 42.65.Ky, 32.80.Rm

The polarization properties of the high-order harmonics (HH) generated in an intense laser field are actively studied both experimentally [1–7] and theoretically [8–10]. These studies show that the harmonics generated in elliptically-polarized laser field are elliptically polarized, and the polarization ellipse of the harmonic is rotated by a certain angle with respect to that of the fundamental (the so-called rotation angle). In addition to the general fundamental interest, studies of high harmonic generation (HHG) in an elliptically polarized field are important in the context of an isolated attosecond pulse production with the ellipticity gating technique [11,12], as well as the generation of elliptically- or circularly polarized coherent XUV.

Many HHG features can be understood in the framework of the well-known ''simple-man'' model [13,14]. It describes HHG as a result of tunneling ionization of the atom by the laser field, free electron motion in this field, and recombination accompanied by the XUV emission upon the return to the parent ion. Thus, this model implies that the direction of the HH field is identical with that of the momentum of the electron coming back to the parent ion and generating XUV photon. However, there is no clear explanation of the origin of the nonzero *ellipticity* of harmonics generated from atoms. The simple-man model predicts zero harmonic ellipticity, which contradicts both the experimental results and those of quantum-mechanical theories.

Note that the perturbation theory predicts a nonzero ellipticity of lower harmonics; however, since HHG is a strongly nonperturbative phenomenon, the results of the perturbation theory [15] can hardly be applied even for a qualitative understanding of the HH ellipticity. The quantum-mechanical theories [8–10] of the process based on the strong-field approximation allow calculation of the ellipticity value. However, no qualitative explanation of the ellipticity origin was suggested within these theories.

In this Letter, we propose the explanation of the origin of the harmonic ellipticity. The explanation is given in terms of the quantum-mechanical spreading of the electronic wave packet after ionization, and of the features of the classical electron trajectories. Simple equations describing the harmonic ellipticity and the rotation angle are derived. These equations are verified by comparison with the numerical solution of the three-dimensional time-dependent Schrödinger equation (TDSE) for a single-electron model atom.

Different electronic quantum paths contribute to the radiating dipole [16]. It was shown theoretically [10,17] that the properties of the contributions of the different quantum paths depend smoothly on the laser field parameters, whereas the dependence of the total microscopic harmonic signal on them is complicated [8,16] due to the interference of the different quantum paths. Our study shows that the above also holds for the polarization state of HH. It is therefore instructive to treat the contributions from different quantum paths separately. Since different trajectories dominate at different time intervals, it allows us to time resolve the sublaser-cycle evolution of harmonic polarization. In our analytical study we will consider for every harmonic only the two most important quantum paths (the ''short'' and the ''long'' ones) which correspond to the travel time τ shorter than one fundamental cycle.

While the numerical TDSE integration allows finding the microscopic response, there is no easy way to separate contributions of different quantum paths in the numerically calculated response. Today we can only refer to a rather complicated indirect technique based on the analysis of the set of numerical TDSE solutions for different intensities [18]. We propose a novel approach to direct separation of the contributions of different quantum paths in the numerical microscopic response. The idea of the approach lies in

suppressing the electron wave function in a certain part of the phase space determined by the position of the relevant classical trajectory in this space. The details of this technique will be described in Ref. [19]. In the present Letter, we extract the contribution of short paths using the frequency-resolved absorption technique [20]. The 3D simulation was done with a fully parallel code "SELAB" [21] for a model argon potential [22]. The separation of the quantum path contributions is illustrated by Fig. 1 showing the scalograms of the responses. We see that the short path's contribution is selected very accurately.

Using the results of the TDSE integration for laser ellipticities up to 0.2 we find the harmonic ellipticity and the rotation angle of the polarization ellipse (also known as offset angle). We find that both quantities depend remarkably linearly on the fundamental's ellipticity, in agreement with experiments [1,4]. The harmonic intensity decreases with the fundamental ellipticity, and the threshold

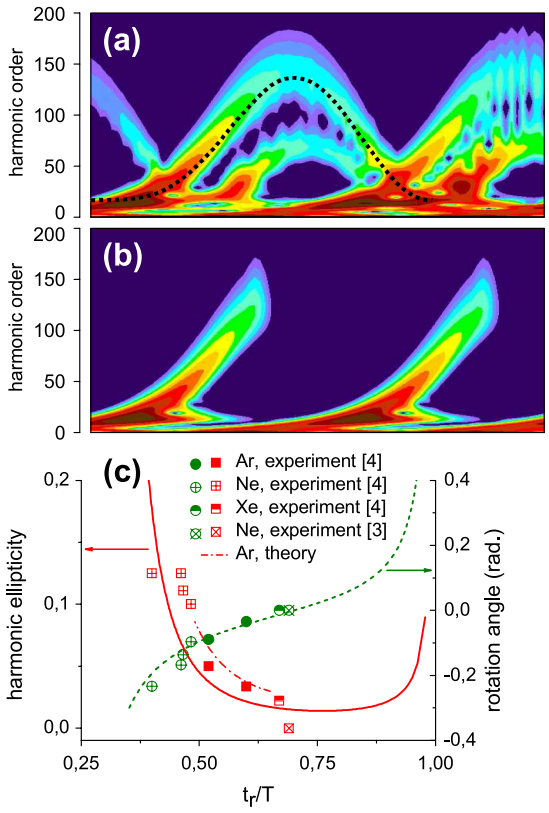

FIG. 1 (color online). Wavelet transform of the numerical atomic response for 1300 nm, 2.2×10^{14} W/cm^2, elliptically-polarized fundamental with ellipticity 0.1: (a) the full response and (b) the contribution of the short quantum path. The dashed line in panel (a) shows the harmonic frequency found within the simple-man model; this curve in fact corresponds to the quantum orbits dominant for the high harmonics. Panel (c) presents the HH polarization properties of dominant contribution found using Eqs. (2) and (5), and experimental data on the rotation angle (green circles) and the upper limit of ellipticity divided by 2 (red squares) from [3,4] (see text for details).

ellipticity (the fundamental ellipticity for which the generation efficiency is 2 times less than for the linearly polarized field) calculated for HHG in Ar with 800 nm laser quantitatively agrees with experiment [11] for different harmonic orders.

Below we derive analytical equations for HH rotation angle and ellipticity. The x and y directions are chosen along the major and minor axis of the fundamental polarization ellipse, respectively. Let $\bar{p}_x$ and $\bar{p}_y$ be the momentum components of the classical electron, which started from the origin with zero velocity, $\bar{y}$ is the transverse shift of this electron, accumulated due to the nonzero fundamental ellipticity by the instant of return to $x = 0$, and τ is the electron excursion time. In the simple-man picture, the HHG is associated with the electron that starts from the origin with the initial y momentum $-\bar{y}/\tau$ and therefore returns exactly to the origin. Thus the "classical" rotation angle is defined by the direction of the electron momentum at the instant of the return

$$\psi_{\text{class}} = \arctan\left[\frac{\bar{p}_y - \bar{y}/\tau}{\bar{p}_x}\right]. \tag{1}$$

Substituting the parameters of the classical electron trajectory [23,24] in this equation we find

$$\psi_{\text{class}} = \varepsilon\left[\frac{1}{\omega\tau} + \frac{\cos(\omega t_r)}{\sqrt{W/(2U)}}\right]. \tag{2}$$

Here ε is the fundamental ellipticity, $U = E^2/(4\omega^2)$ is the ponderomotive energy and W is the kinetic energy of the returning electron. This energy is related to the harmonic order by $W = q\omega - I$, where I is the ionization energy. The electron return instant t_r, the ionization instant t_i, and τ can be found from W as described in [23,24].

The rotation angle can be found more accurately taking into account quantum-mechanical features of the electron motion. To do this, we use complex amplitudes of the x and y components of the harmonic response f_x and f_y found in [10] [Eqs. (33),(34)]. Defining the rotation angle as $\psi_{q-m} = \arctan\text{Re}[f_y/f_x]$ we find

$$\psi_{q-m} = \varepsilon\left[\frac{\cos(\omega t_i) - \omega\tau\sin(\omega t_i)(1 + \frac{4}{\tau^2\Delta p_\perp^4}) + \frac{\sqrt{W/(2U)}}{\omega\tau}}{\sqrt{W/(2U)}(1 + \frac{4}{\tau^2\Delta p_\perp^4})}\right], \tag{3}$$

where $\Delta p_\perp$ is the uncertainty of the transverse electronic momentum after ionization: $\Delta p_\perp^2 = 2IE\cos(\omega t_i)$ [25].

Figure 2(a) shows the rotation angle as a function of the harmonic order for $0 < \tau < 2\pi/\omega$ found from the described approximations as well as from the numerical simulation for the short quantum path. The analytical results agree well with the numerical ones, except lowest-order harmonics (this disagreement is natural because they can hardly be described via strong-field approximation). For the higher harmonics the

quantum-mechanical approach gives better results than the classical one.

As for the harmonic ellipticity, it cannot be described with a classical model, as discussed above. We define the harmonic ellipticity as $\epsilon = \arctan\mathrm{Re}[if_y/f_x]$. Using f_x and f_y from [10] we find

$$\epsilon = \frac{\bar{y}}{\bar{p}_x[\tau^2\Delta p_\perp^2/2 + 2/\Delta p_\perp^2]}, \tag{4}$$

and substituting the parameters of the classical electron motion in this equation we find for $\omega\tau 2I\sqrt{U} \gg 1$:

$$\epsilon = \varepsilon/(I\omega\tau\sqrt{2W}). \tag{5}$$

Figure 2(b) shows the harmonic ellipticity calculated numerically, as well as one found analytically with the latter equation. One can see that the analytical quantum-mechanical approximation provides very good agreement with numerical results for almost all harmonics except the lowest-order ones. Note that ellipticities of the both quantum paths contributions have the same sign as the fundamental has (i.e. the instantaneous harmonic field vector rotates in the same direction as the fundamental one does). However, in the *total* numerical response few harmonics have opposite ellipticity, as it was earlier reported in [8]. Our studies show that this anomalous ellipticity originates from the contributions of the quantum paths with the excursion time exceeding optical cycle.

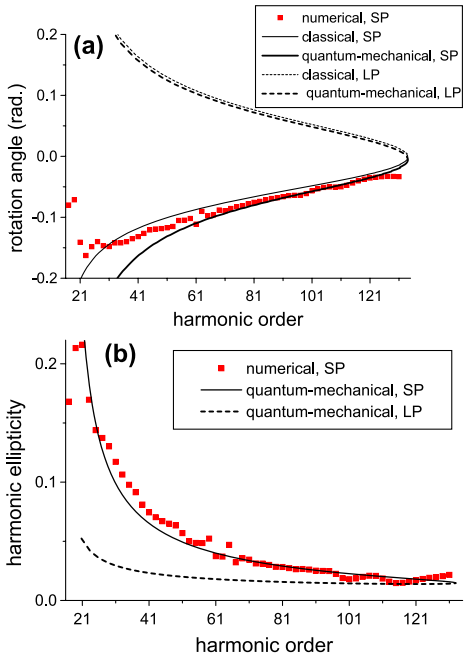

FIG. 2 (color online). Harmonic rotation angle (a) and ellipticity (b) as functions of the harmonic order, the laser parameters are the same as in Fig. 1. Numerical results for the short quantum path (squares), analytical quantum-mechanical results given by Eq. (3) (graph a) and Eq. (5) (graph b) for the short (solid line) and the long (dashed line) quantum path. Graph (a) presents also classical rotation angle given by Eq. (2).

Thus, our theoretical approach provides quantitative agreement with numerical results. Moreover, it enables calculation of the temporal sublaser-cycle evolution of the XUV polarization state [see Fig. 1(c)]. In this figure we also present experimental results [3,4]. Note that the harmonic ellipticity upper limit, but not the ellipticity itself was measured in [4] due to experimental limitations. Although obtained for different media, harmonic orders, fundamental intensities and wavelengths, the experimental results demonstrate clear tendency if presented as functions of the classical electron return time, reconstructed for every experimental point. The polarization properties calculated as functions of this time for conditions of these experiments are very close to each other, except the ellipticity for Ar which, for the conditions of [4], is therefore shown separately with the dash-dotted line. The harmonic rotation angle agrees very well with the analytical result, and the ellipticity upper limit is about 2 times higher than the ellipticity found from our model.

Our approach allows qualitative understanding of the harmonic ellipticity origin as well. From Eq. (4) one can see that the harmonic ellipticity originates from the quantum-mechanical uncertainty of the transverse electronic momentum. This nonzero uncertainty corresponds to the finite size of the wave packet. When the wave packet traveling near the parent ion is shifted in the transverse direction (by the displacement $\bar{y}$), the parent ion ''sees'' a slope of the population density in the wave packet: the population density grows towards the packet center. This asymmetry finally leads to a certain y component of the dipole oscillating with a $\pi/2$ phase shift with respect to the x component, and thus to the harmonic ellipticity.

To illustrate these speculations in more detail, let us consider a bound state $\psi_0(x, y, z) = \psi(x)\psi(y)\psi(z)$ (where ψ is an even function) and a free electronic wave packet moving along the x coordinate $\chi(x, y, z) = f(y, z) \times \exp(ipx)$. Assume that the maximum of the amplitude $f(y, z)$ is shifted in the y direction, so the amplitude can be expanded in the Taylor series in the vicinity of the origin as $f = f_0 + f_1 y$. The dipole moment of the system is $\mathbf{d} = \int \psi_0^* \mathbf{r}\chi d\mathbf{r}$ + c.c. For its x and y components we find $d_x \propto f_0$ and $d_y \propto if_1$. Thus the phase difference between oscillations of the two components is $\pi/2$, i.e., the total signal is elliptically polarized, and the ellipticity is proportional to the slope of the population density of the wave packet in the y direction.

Note that a factor proportional to this slope appears already in (4). Indeed, consider a Gaussian wave packet with the size $\tau^2\Delta p_\perp^2/2 + 2/\Delta p_\perp^2$. The slope of its amplitude is

$$\frac{\partial}{\partial y}\exp\left(-\frac{y^2}{\tau^2\Delta p_\perp^2/2 + 2/\Delta p_\perp^2}\right) \propto \frac{y}{\tau^2\Delta p_\perp^2/2 + 2/\Delta p_\perp^2}.$$

Note that in this Letter we do not take into account Coulomb effects. Good agreement of the analytical and numerical results shows that the Coulomb effects are not responsible for the harmonic ellipticity, at least for the short quantum path and not very low harmonic orders.

The nonzero ellipticity of the generated radiation appears in other processes involving electron-ion recombination (e.g., in the HHG by cross-polarized fields with different colors). To describe the polarization properties of the generated radiation one should substitute the parameters of the classical electron trajectory (in such field) in Eqs. (1) and (4). The simplicity of our model can allow, in particular, finding the field configuration providing XUV with the desired polarization properties. Our model can be generalized to find the polarization properties of the HHG from molecules, actively studied experimentally [5–7]. For instance, to calculate the y component of the emitted radiation for a diatomic homonuclear molecule one can apply our approach in conjunction with the two-center model [26]. If the molecular axis is nonparallel to the polarization direction, the returning electron wave packet slightly misses every of the centers (even in the linearly polarized fundamental), and thus the y component from every center appears. For the perpendicular orientation these contributions compensate each other, but for different orientation their interference leads to nontrivial behavior of the harmonic polarization properties. For the total y component we find $d_y^{\mathrm{mol}} \propto \sin(p_x R\cos(\theta)/2)\sin(\theta)$ where θ is the angle between the molecular axis and the polarization direction, and R is the internuclear distance. This dependence agrees very well with experimental results showing maximal intensity of the y component [6] and maximal ellipticity [6,7] for $\theta \approx 50^0$ for different harmonics in N_2. Further results on the generalization of our approach to the molecular case will be presented in [19].

Moreover, our model can be useful for understanding of the polarization of light emitted with coherent wave packets even beyond the recombination, for instance, in the ''wave-packet-spreading'' regime [27], or in the dynamic stabilization regime [28].

In conclusion, in this Letter, based on the detailed numerical and analytical study of the polarization properties of the harmonics, we offer an explanation for the origin of the ellipticity of the harmonics generated in atomic gases by elliptically polarized laser fields. The harmonic ellipticity results from the limited size of the electronic wave packet coming back to the parent ion and generating harmonics: the ellipticity naturally appears when the center of the wave packet misses the parent ion. We have also derived very simple analytical equations describing HH polarization properties, which agree well with the numerical results for the short quantum path. These equations allow, in particular, clear description of the sub-laser-cycle evolution of the XUV polarization state. Our model can be generalized to study HHG in the cross-polarized fields of different colors, as well as HHG from molecules. We believe that the achieved understanding of the harmonic ellipticity in the recombination process can be useful for study of other recollision-induced phenomena involving light emission with coherent wave packets.

We acknowledge the Joint Supercomputer Center of RAS for the provided supercomputer sources. This study was supported by RFBR, Presidential Council on Grants of RF (MD-5752.2010.2, NS-3800.2010.2), and the Ministry of Education and Science of RF.

*v-strelkov@fpl.gpi.ru

[1] F. A. Weihe *et al.*, Phys. Rev. A **51**, R3433 (1995).
[2] F. A. Weihe and P. H. Bucksbaum, J. Opt. Soc. Am. B **13**, 157 (1996).
[3] D. Schulze *et al.*, Phys. Rev. A **57**, 3003 (1998).
[4] Ph. Antoine *et al.*, Phys. Rev. A **55**, 1314 (1997).
[5] J. Levesque *et al.*, Phys. Rev. Lett. **99**, 243001 (2007).
[6] X. Zhou *et al.*, Phys. Rev. Lett. **102**, 073902 (2009).
[7] Y. Mairesse *et al.*, Phys. Rev. Lett. **104**, 213601 (2010).
[8] Ph. Antoine *et al.*, Phys. Rev. A **53**, 1725 (1996).
[9] B. Borca *et al.*, Phys. Rev. Lett. **85**, 732 (2000).
[10] V. V. Strelkov, Phys. Rev. A **74**, 013405 (2006).
[11] I. J. Sola *et al.*, Nature Phys. **2**, 319 (2006).
[12] G. Sansone *et al.*, Science **314**, 443 (2006).
[13] P. B. Corkum, Phys. Rev. Lett. **71**, 1994 (1993).
[14] K. J. Schafer *et al.*, Phys. Rev. Lett. **70**, 1599 (1993).
[15] N. L. Manakov and V. D. Ovsyannikov, Zh. Eksp. Teor. Fiz. **79**, 1769 (1980) [Sov. Phys. JETP **52**, 895 (1980)].
[16] M. Lewenstein *et al.*, Phys. Rev. A **49**, 2117 (1994).
[17] V. T. Platonenko, Quantum Electron. **31**, 55 (2001).
[18] M. B. Gaarde and K. J. Schafer, Phys. Rev. A **65**, 031406 (R) (2002).
[19] V. V. Strelkov *et al.* (to be published).
[20] A. A. Gonoskov and I. A. Gonoskov, arXiv:physics/0607120.
[21] http://www.ipfran.ru/english/structure/lab334/simlight.html.
[22] V. V. Strelkov, V. T. Platonenko, and A. Becker, Phys. Rev. A **71**, 053808 (2005).
[23] V. T. Platonenko and V. V. Strelkov, Quantum Electron. **28**, 564 (1998).
[24] W. Becker *et al.*, Adv. At. Mol. Opt. Phys. **48**, 35 (2002).
[25] A. M. Perelomov, V. S. Popov, and M. V. Terent'ev, Zh. Eksp. Teor. Fiz. **50**, 1393 (1966) [Sov. Phys. JETP **23**, 924 (1966)].
[26] M. Lein *et al.*, Phys. Rev. A **66**, 023805 (2002).
[27] M. V. Fedorov and J. Peatross, Phys. Rev. A **52**, 504 (1995).
[28] M. Yu. Ryabikin and A. M. Sergeev, Laser Phys. **12**, 757 (2002).